Electronic Supplementary Material (ESI) for Physical Chemistry Chemical Physics.
This journal is © the Owner Societies 2016

Electronic Supplementary Information

Fabrication of mixed phase TiO_2 heterojunction nanorods and its enhanced photoactivities

Amritanjali Tiwari,[a,b] Indranil Mondal,[a,b] Saptarshi Ghosh,[d] Nitin Chattopadhyay,[d] Ujjwal Pal*[a,b,c]

[a]*Central Mechanical Engineering Research Institute, M. G. Avenue, Durgapur-713209, WB, India.*

[b]*Network of Institutes for Solar Energy (CSIR-NISE) and Academy of Scientific and Innovative Research (AcSIR).*

[c]*Inorganic and Physical Chemistry Division, CSIR-Indian Institute of Chemical Technology, Hyderabad*

[d]*Department of Chemistry, Jadavpur University, Kolkata 70032, India*

Corresponding Author

*Ujjwal Pal, E-mail: upal03@gmail.com; Fax: (+91) 343-2546745.

Structural characterization

Powder X-ray diffraction patterns (XRD) of the photocatalysts were recorded on a Bruker AXS diffractometer (D8 advance) at a generator voltage of 40 kV and current 30 mA using Cu-Kα radiation (λ = 1.5406 Å). The sample was scanned in the range of 2θ = 5-100° with the scan rate 1 s/step. N_2 adsorption–desorption isotherms of the photocatalysts were obtained on a Quantachrome Nova 2200e gas adsorption analyzer at 77 K. Field emission scanning electron microscopy (FESEM) was performed on a Carl Zeiss SIGMA HD field-emission scanning electron microscope. Transmission electron microscopy (TEM) image of the representative TNR sample was obtained by using a JEOL 2010EX TEM instrument equipped with the high-resolution style objective-lens pole piece at an acceleration voltage of 200 kV fitted with a CCD camera. Raman spectra was collected using J–Y Horiba Confocal Triple Raman Spectrometer (Model: T64000) fitted with gratings of 1800 groove/mm, and a TE cooled Synapse CCD detector from J–Y Horiba. 632.8 nm red line of He–Ne laser was made up by Melles Griot. The scattered signals were collected at 1800 scattering angle to the excitations from an Olympus open

stage microscope. UV-vis diffuse reflectance spectra (UV-vis DRS) was obtained on Lab sphere DRA-CA-3300 compartment associated with the Varian Cary 100 spectrophotometer over 250-800 nm range using $BaSO_4$ as a reference. The Kubelka-Munk function F (R∞) (which is equivalent to the absorbance) was plotted against wavelength, and band gap values were calculated by extrapolating the lower wavelength cut-off region. Photoluminescence spectra of the as-prepared samples are suspended in aqueous solution (pH 7) without using any solvent. The spectra were measured with fluorescence spectrophotometer by Cary eclipse fluorescence spectrometer from Agilent Technologies, excitation at 370 nm (the intensity was normalized). The photocatalytic experiments were carried out under external light source using a 450 W xenon arc lamp (Newport, USA and working at 400 W). GC analysis was performed by Perkin-Elmer gas chromatograph Clarus-580 instrument with a thermal conductivity detector and a 5Å molecular sieve column (2 mm × 2 mm) using Argon as carrier gas.

The conditions of XRD data collection are as given below:

Scan Axis:	Gonio
Start Position (°2θ):	5
Start Position (°2θ):	95
Step Size (°2θ):	0.0500
Anode material:	Cu
Generator setting:	40 mA, 40 kV

Synthesis: In the study, the results demonstrate that the as-prepared nonaqueous solvothermal process enables highly flexible manipulation of the structure and morphology of TiO_2 nanomaterials by reaction of TBOT with different concentration of $TiCl_4$ in toluene. The synthesis routes of the photocatalysts are described as follows (Scheme S1).

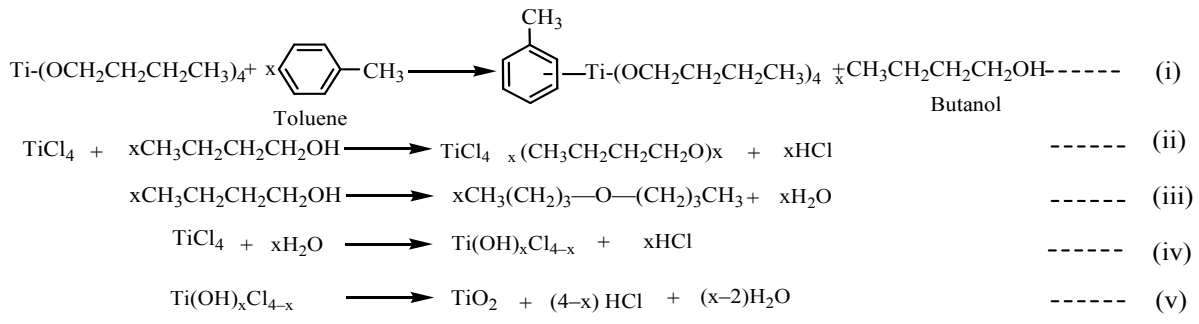

Scheme S1. Plausible mechanism for the preparation of TiO_2

When Ti-$(OCH_2CH_2CH_2CH_3)_4$ reacts with toluene, it produces toluene-Ti-$(OCH_2CH_2CH_2CH_3)_{4-x}$ complex and butanol. Further, $TiCl_4$ reacts with butanol, produces $TiCl_{4-x}(CH_3CH_2CH_2CH_2O)_x$, $CH_3CH_2CH_2CH_2Cl$ and HCl. The hydrolysis of $TiCl_4$ gives different $Ti(OH)_{4-x}Cl_x$ species which at elevated temperature, undergoes polycondensation, the formation of Ti-O-Ti network. The resulting anatase and rutile heterojunction nanorods and anatase phase of nanoparticles are selectively produced through controlled addition of TBOT and $TiCl_4$ by adjusting their volume ratio. The plausible reason may be that higher volume ratio of $TiCl_4$ produces a steric hindrance in mixture solution that serves as a barrier against the hydrolysis and increases the growth of TiO_2 nanocomposite with a good crystallinity.

Photocatalytic dye degradation

RhB and MB were chosen to measure photocatalytic performance of the **ART-I**, **ART-II**, **ART-III**, **AT** and **RT** photocatalysts under full arc irradiation. In a typical measurement, 10 mg of each photocatalyst was suspended in 30 mL of 1 x 10^{-5} M aqueous solution of RhB and MB dyes. The solution was stirred in the dark for 30 minute to achieve the equilibrium adsorption. The suspension was then illuminated with a 450 W xenon lamp (working at 400 W). At appropriate intervals, withdraw 3 mL of suspension, centrifuge, and remove the photocatalyst. Monitor the concentration of RhB and MB solution using UV−vis spectrophotometer. The photodegradation kinetics were fitted to a pseudo-first-order reaction, ($C_0/C = e^{kt}$), where k is the apparent rate constant.

Linear scan voltammetry Measurement

Linear scan voltammetry (LSV) measurement was performed on a CHI 600E electrochemical workstation system. The testing system was comprised of three electrodes, a single-compartment quartz cell filled with 0.2 M Na_2SO_4 electrolyte (10 mL), a Pt disk counter electrode and Ag/AgCl reference electrode. A thin film of TNR composites with the same area of 3 cm^2 was employed as a working electrode. A 450 W xenon arc lamp (Newport, USA, model no: 66924; working at 400 W) was used as the exciting light source for UV-vis light irradiation.

Time-resolved photoluminescence

Photoluminescence lifetimes were determined from the time-resolved fluorescence decays by the method of time-correlated single photon counting (TCSPC) using excitation source at 370 nm (Nano LED) with TBX-04 detector (both IBH, UK). The instrument response time was ~1 ns. The instrument response function was collected by placing a scatterer (dilute micellar solution of sodium dodecyl sulfate in water) in place of the sample. The decays were analyzed using IBH DAS-6 decay analysis software. Goodness of the fits was evaluated from the $\chi 2$ criterion (which were in the range 1.0 -1.2) and visual inspection of the randomness of the residuals of the fitted function to the data. Mean fluorescence lifetimes (τ_f) of the samples are calculated from the decay times (τ) and their corresponding pre-exponentials (a) using the following relation

$$< \tau_f > = \sum a_i \tau_i$$

Table S1. Compositions of the solutions for solvothermal reaction of TiO_2 nanorods and nanoparticles synthesized under different conditions

Sample	TBOT (mL) d=1 mL/g	$TiCl_4$ (mL) d=1.73 mL/g	Mass ratio of $TiCl_4$: TBOT	HCl (mL)	Toluene (mL)
ART-I	1	0	0:1	0.5	10
ART-II	1	0.25	0.43:1	0.5	10
ART-III	1	1	1.73:1	0.5	10
AT	1	4	6.92:1	0.5	10

Table S2. Surface analysis data

Sample	Specific surface area (m^2 g^{-1}) [a]	Average pore size (nm) [b]	Pore volume (cm^3 g^{-1})
ART-I	54.58	18.13	0.177
ART-II	67.08	18.94	0.211
ART-III	69.15	18.34	0.218
AT	53.63	18.72	0.231

[a] Specific surface area was calculated from the linear part of BET plot. [b] Average pore diameter was estimated.

Table S3. Fluorescence lifetime values for the samples

Sample	Lifetime (ns)
ART-I	0.192
ART-II	0.487
ART-III	0.312
AT	0.220
RT	0.138

Table S4. Photocatalytic H_2 evolution

Material	Cocatalyst	Light source[a]	Reaction solution[b]	H_2 Activity (mmol g^{-1} h^{-1})	Reference (year)
TiO_2	Pt	UV-Vis (Xe) 300 W	Methanol	0.425	1 (2010)
TiO_2	Pt	UV-Vis (H) 150 W	TEOA	3.66	2(2012)
TiO_2	Au	UV-Vis (Hg) 300 W	Methanol	2.78	3 (2005)
TiO_2	$Cu(OH)_2$	UV-Vis (Hg) 400 W	Methanol	14.9	4 (2013)
TiO_2	$Ni(OH)_2$	365 nm (LED) 3 W	Methanol	3.05	5 (2011)
TiO_2	MoS_2–RGO	UV-Vis (Xe) 350 W	Ethanol	2.06	6 (2012)
TiO_2	NiO	UV-Vis (Hg) 300 W	Methanol	0.81	7 (2005)
TiO_2	**Pt**	**UV-Vis (Xe) 400 W**	**Methanol**	**16.4**	**This work**

[a]H: halogen lamp, Xe: xenon lamp, Hg: mercury lamp.

[b]TEOA: triethanolamine.

Table S5. Comparison of the photocatalytic degradation efficiency of various catalysts

Photocatalyst	Reaction condition	Irradiation Time (min)	Percentage degradation of MB and RhB	Reference
RhB-W4	20 mg of the TiO_2 catalyst was dispersed in a 30-mL RhB solution, 350 W (15 A) Xenon lamp	90	92.4	8
RhB-P25	1 x 10^{-5} mol L^{-1} RhB and 10 mg catalyst, 150 W high pressure Hg lamp	60	65	9
RhB- TiO_2-200	20 mg catalyst and 50 mL of RhB solution with a concentration of 10 mg L^{-1}, 22 W visible-light lamp, <400 nm	300	96.8	10
MB-pristine TiO_2	30 mg catalyst, 50 ml deionozed water, 0.01 g/L (MB) aq. solution, Xe lamp (AM 1.5 G and 100 mW cm^{-2})	20	23.5	11
MB-T400	ultraviolet (UV) lamp (λ_{max} = 312 nm, 30 W)	360	92	12
MB-P25	10 mg/L MB in 0.1 M Na_2S solution. Xe lamp (AM 1.5 G and 100 mW/cm^2)	240	19	13
MB-ART-II	10 mg catalyst, 1 x 10^{-5} M MB, 450 W Xe lamp (working at 400 W)	60	90	**This work**
RhB-ART-II	10 mg catalyst, 1 x 10^{-5} M RhB, 450 W Xe lamp (working at 400 W)	60	95	**This work**

Methylene blue (MB) and Rhodamine B (RhB)

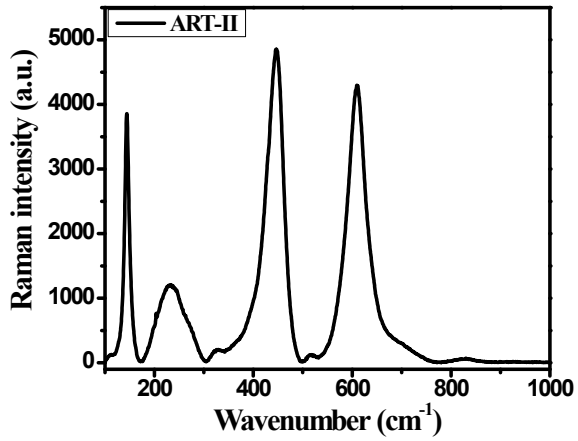

Figure S1. Raman spectrum band of ART-II

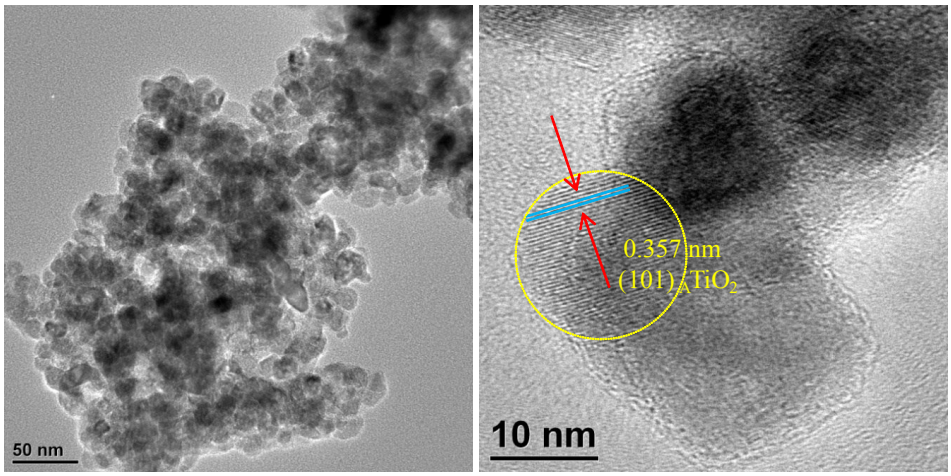

Figure S2. TEM image of **AT**

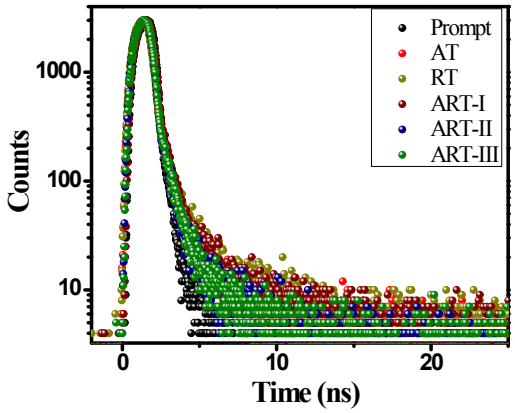

Figure S3. Time-resolved photoluminescence spectra of **ART-I, ART-II, ART-III, AT** and **RT,** excitation (λ_{exc}) at 370 nm.

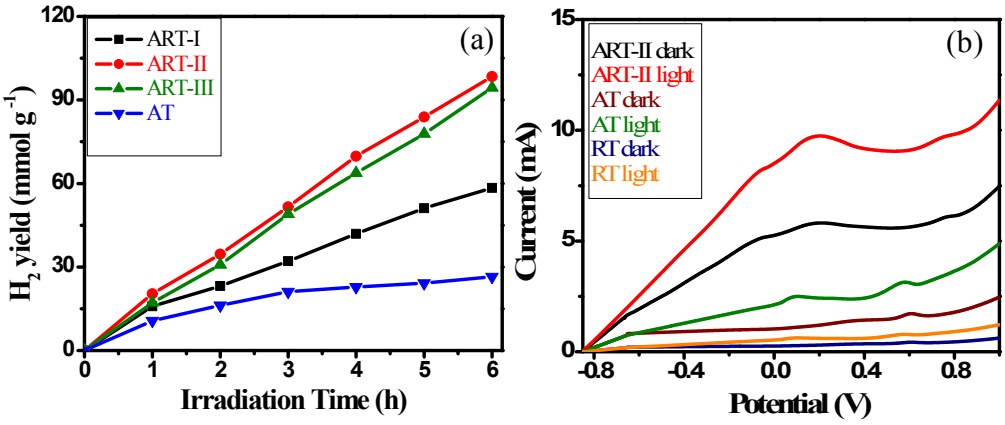

Figure S4. (a) Time course of photocatalytic H_2 generation of different TiO_2 samples; (b) LSV of different TiO_2 samples

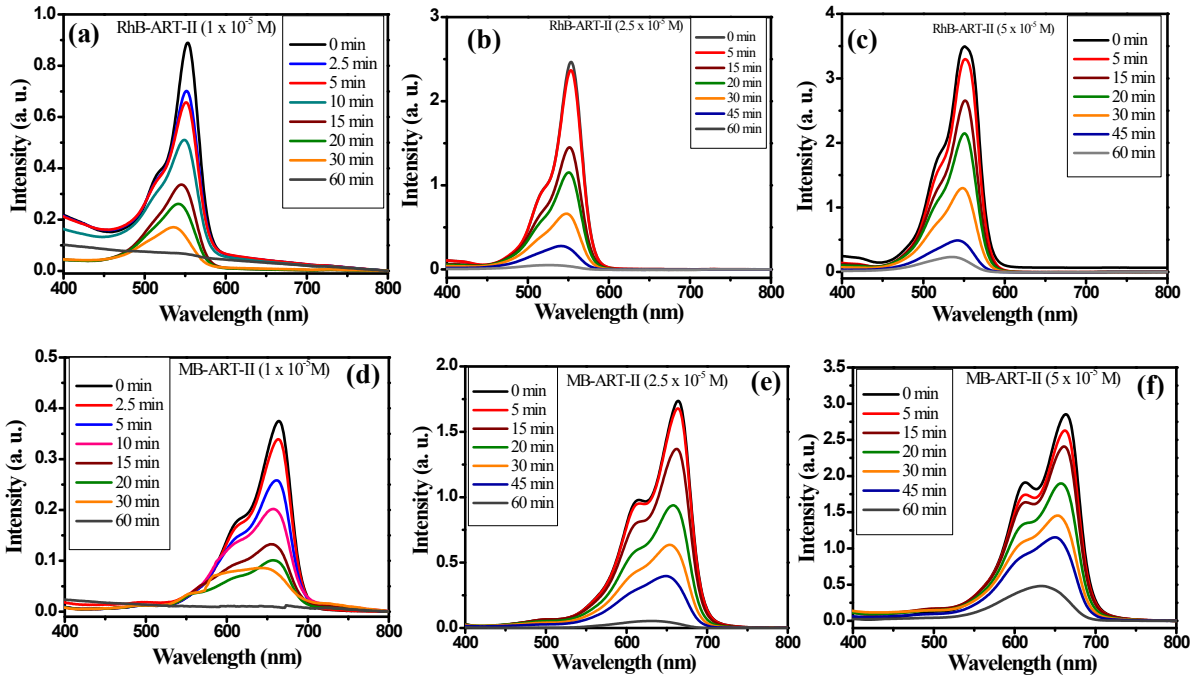

Figure S5 Absorption spectral changes of (a-c) RhB and (d-f) MB dyes solution with different concentration under full arc light irradiation in the presence of **ART-II** photocatalyst.

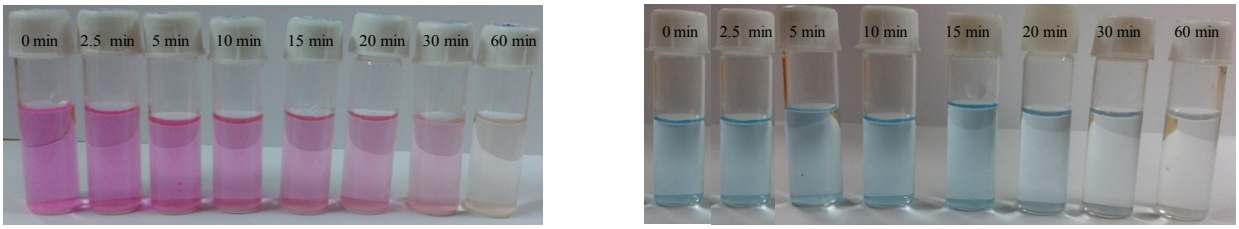

Figure S6. Colour changes of RhB and MB (dye concentration 1 x 10^{-5} M) under full arc light irradiation in the presence of **ART-II** catalyst for different time lengths.

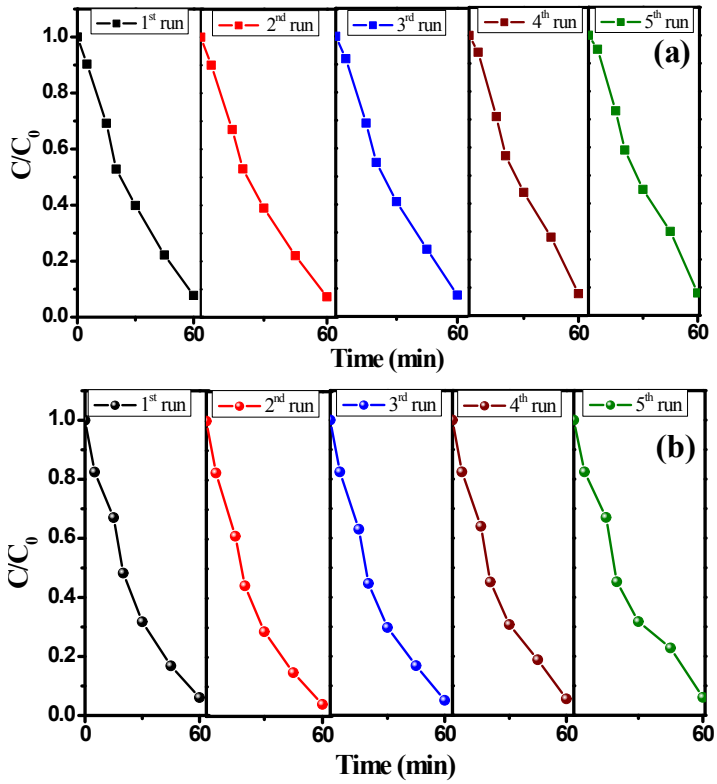

Figure S7. Repeated photocatalytic experiments of (a) MB and (b) RhB with ART-II

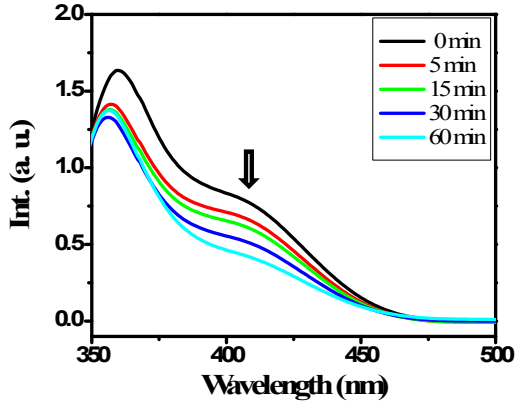

Figure S8. Photocatalytic degradation profile of 4-NP in presence of ART-II.

References

1. Y. K. Kho, A. Iwase, W. Y. Teoh, L. Ma¨dler, A. Kudo, R. Amal, *J. Phys. Chem. C,* 2010, **114,** 2821.
2. P. D. Tran, L. F. Xi, S. K. Batabyal, L. H. Wong, J. Barber, J. S. C. Loo, *Phys. Chem. Chem. Phys*., 2012**, 14,** 11596.
3. T. Sreethawong, S. Yoshikawa, *Catal. Commun.* 2005, **6***,* 661.
4. H. F. Dang, X. F. Dong, Y. C. Dong, Y. Zhang, S. Hampshire, *Int. J. Hydrogen Energy,* 2013, **38**, 2126.
5. J. G. Yu, Y. Hai, B. Cheng, *J. Phys. Chem. C,* 2011, **115,** 4953.
6. Q. J. Xiang, J. G. Yu, M. Jaroniec, *J. Am. Chem. Soc.,* 2012, **134,** 6575.
7. T. Sreethawong, Y. Suzuki, S. Yoshikawa, *Int. J. Hydrogen Energy*, 2005, **30,** 1053.
8. W.-K. Wang, J.-J. Chen, X. Zhang, Y.-X. Huang, W.-W. Li and H.-Q. Yu, *Sci. Rep*., 2015, **6**, 20491.
9. S. Li, J. Chen, F. Zheng, Y. Li and F. Huang, *Nanoscale*, 2013, **5**, 12150.
10. X. Liu, Y. Li, D. Deng, N. Chen, X. Xing and Y. Wang, *Cryst Eng Comm*., 2016, **18**, 1964.
11. R. Ren, Z. Wen, S. Cui, Y. Hou, X. Guo and J. Chen, *Sci. Rep*., 2015, **5**, 10714.
12. M. A. Mohamed, W. N. W. Salleh, J. Jaafar and A. F. Ismail, *J. Sol-Gel Sci. Technol*., 2015, **74**, 513.
13. C. J. Lin, Y. H. Yu and Y. H. Liou, *Appl. Catal. B: Environ*., 2009, **93**, 119.